Electronic Supplementary Material (ESI) for Chemical Science.


# Electronic Supplementary Information

## Intermolecular Noncovalent Interactions with Carbon in Solution

## Computational Details

### Molecular Dynamics (MD) Simulations

The charges for chloroform, pyridine N-oxide (PNO) and 3,3-dimethyl-1,1,2,2-tetracyanocyclopropane (DMTCCP) were derived by restrained electrostatic potential (RESP) method[1] to fit the B3LYP/6-31+G** charges calculated with the Gaussian 09 program[2]. The topology files were generated with the Antechamber module[3] in AMBER 14[4]. This methodology is in accordance with the GAFF (Generalized Amber Force Field)[5] parameterization.

The MD simulations were performed with the sander program of the AMBER 14 package. All the simulations employed periodic boundary conditions. The PME (Particle Mesh Ewald)[6] was used to calculate electrostatic energy. All the bonds were constrained using the SHAKE[7] algorithm, which allowed us to use a higher time step of 2 fs. Langevin dynamics was used to regulate the temperature with a collision frequency of 5 $ps^{-1}$.[8] Isotropic scaling was implemented for pressure regulation associated with a pressure relaxation time of 1 ps. Prior to data collection, the systems were energy minimized and equilibrated. After energy minimization, the system was equilibrated for 1 ns under NVT. The system was equilibrated under NPT at a constant pressure of 1 bar for 5 ns in the following stage. This was followed by a production run, which was run under similar conditions as the previous equilibration phase under NPT.

The production trajectory was 40 ns long for the PNO-DMTCCP system. The PNO-DMTCCP system contained 1 DMTCCP, 40 PNO and 512 chloroform molecules. The various analyses were carried out using the cpptraj module[9] of AMBER 14 and TRAVIS[10].

To calculate the diffusion co-efficients, we have sampled the mean squared displacements (MSD) of the molecules from 20 independent sampling simulation runs (each 2 ns long) starting from the same initial coordinates.[11] The diffusion coefficient can be calculated from the slope of the plot between the MSD of the required species versus simulation time by using equation-S1. The independence of the 20 MD runs was achieved by using different random seeds used for the generation of initial velocities.

$$MSD = 2nDt \qquad \textbf{(S1)}$$

where, $n$ is the number of dimensions in which the MD simulations were performed (in our case, n = 3), $D$ is the diffusion coefficient, and $t$ is time.

Least square fitting the mean MSD versus time data for DMTCCP in $CHCl_3$ and PNO-DMTCCP in $CHCl_3$ in Figure 4d yielded the following equations, respectively:

$$y = 0.21x - 6.88,\ R^2 = 0.99 \text{ (for DMTCCP in } CHCl_3\text{)} \quad \textbf{(S2)}$$

$$y = 0.15x + 20.66,\ R^2 = 0.99 \text{ (for PNO-DMTCCP in } CHCl_3\text{)} \quad \textbf{(S3)}$$

where $R^2$ is the correlation coefficient.

The value $\mathbf{D_{DMTCCP}/D_{PNO\text{-}DMTCCP}}$ was computed as the ratio of the slope of equation-S2 to the slope of equation-S3, giving a value of 1.40.

**Distribution functions**

Although we could visualize the maximum probability of finding PNO around DMTCCP through the spatial distribution function (SDF) in Figure 2 in the main text, we have calculated various other distribution functions to get a more concrete picture of the arrangement of the PNO molecules.

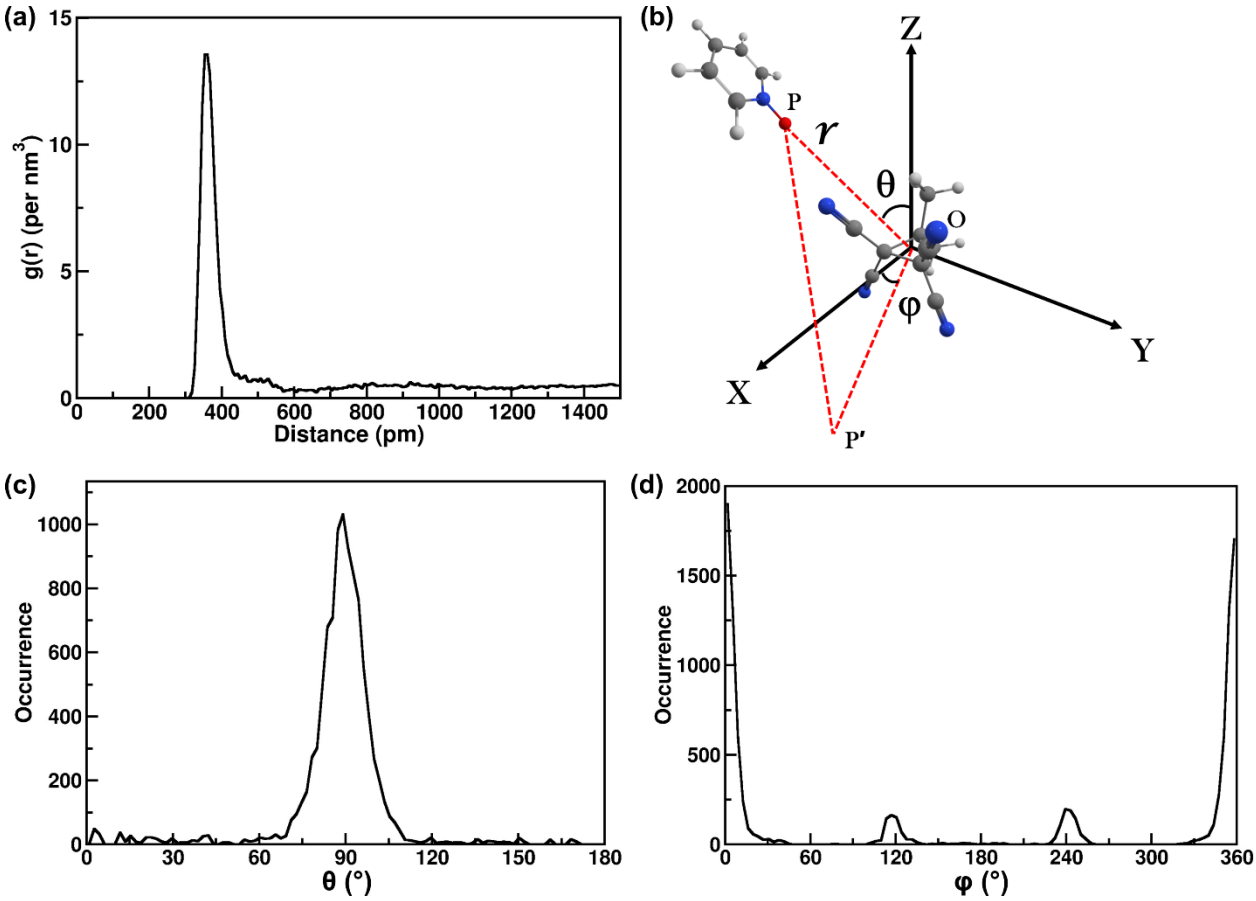


***Figure S1. (a)*** *Radial distribution function (RDF) between the oxygen atom of PNO molecules and the centre of the ring (COR) of DMTCCP.* ***(b)*** *The spherical coordinate system is used as a reference for distribution functions presented in the following figures.* ***(c)*** *Angular distribution function (ADF) of the polar angle θ of the nearest neighbouring PNO molecules of DMTCCP* ***(d)*** *Angular distribution function (ADF) of the azimuthal angle φ for the nearest neighbouring PNO molecules of DMTCCP.*

These include the RDF from Figure 2b and the ADFs from Figures S1c and S1d. To understand these distribution functions, we used a spherical coordinate system (Figure S1b). The origin O of the coordinate system is placed at the centre of the ring (COR) of DMTCCP with the ring of DMTCCP in the XY plane. The radial distance r is the distance between COR of DMTCCP and the oxygen atom of PNO (OP). The polar angle θ is defined as the angle between the zenith direction ($\hat{Z}$) and the line OP (line joining the centre of the ring and the oxygen atom of PNO), and the azimuthal angle φ is the angle between the azimuth reference direction ($\hat{X}$) and the projection of the line OP on the XY plane (OP′). It is also important to note that OX bisects the side of the cyclopropane ring containing the two carbon atoms substituted with the four nitrile groups. Having explained the coordinate system, we move to the various distribution functions. Figure S1c shows the distribution of the polar angle θ for the nearest neighbouring PNO

molecules of DMTCCP. The peak is centred ~90° which shows that the oxygen atom of the PNO molecule approaches the DMTCCP along the plane of the ring of DMTCCP.

Further, we have calculated the azimuthal angle distribution φ for the nearest neighboring PNO molecules of DMTCCP (Figure S1d). The prominent peaks near ~0° and ~360° show that the oxygen atom of PNO primarily approaches the DMTCCP along the region flanked by the four nitriles (corresponds to the large isosurface in the SDF in Figure 2c). The small peaks near ~120° and ~240° are contributed by the PNO molecules approaching the other two sides of the cyclopropane ring (corresponds to the small spheres on the two sides of the cyclopropane ring not containing the nitrile pocket in the SDF in Figure 2c).

**Quantum Mechanical Calculations**

The monomers and PNO:DMTCCP complex structures were optimized at the RI-B97D3/def2-TZVPP level of theory, and the single point energy was calculated at the gold standard CCSD (T)/def2-TZVPP level of theory in chloroform using Cosmoprep module in Turbomole V7.2 software package[12]. The molecular electrostatic potential surface for the DMTCCP was calculated at the MP2/def2TZVPP level of theory and the surface was mapped with the isovalue of 0.001 a.u. within the colour range of -0.05 a.u. to +0.05 a.u with the help of GaussView 6 software[13]. The natural bond orbital (NBO) calculations were performed at the MP2/def2TZVPP level of theory using NBO-3.0 programme[14] in Gaussian-16 software package[15]. The computational NMR was performed at the B3LYP/def2TZVPP level of theory in the Gaussian-16 software package. It is worth to mention that the polarisable continuum model was used to include the solvent ($CHCl_3$) effect to the systems.

We also optimized one structure of PNO-DMTCCP complex where PNO is directed towards the methyl group. In **Figure 1d** in the main manuscript, the methyl groups also show the positive potential region. But the interaction energy is -5.59 kJ/mol, which is too low for the homodimer to be detected in the solution phase. Thus the most probable structure would be the structure mentioned in **Figure 3a**.

Thermodynamical parameters (H and ΔH) in solution at CCSD(T) level were calculated as follows:

The $H^{CCSD-T}$(sol) was calculated from the equation given below[16]:

$$\mathbf{H^{CCSD-T}(sol) = E^{CCSD-T}(gas) + H^{B97-D}\ (sol) + ZPE^{B97-D}\ (sol) + [E^{B97-D}\ (sol) - E^{B97-D}\ (gas)]}$$

To calculate the change in enthalpy upon complex formation, we used the following equation:

$$\Delta H^{CCSD\text{-}T}\,(sol) = H^{CCSD\text{-}T}(sol)_{PNO\text{-}DMTCCP} - [H^{CCSD\text{-}T}(sol)_{DMTCCP} + H^{CCSD\text{-}T}(sol)_{PNO}]$$

**Table S1:** Details of NBO Analysis

| Orbital Contribution | $\Delta E^2$ (kJ/mol) | Contribution (%) |
|---|---|---|
| LP(1)$O_{20}$ → π*$C_4$-$N_5$ | 1.76 | 29 |
| LP(2)$O_{20}$ → π*$C_4$-$N_5$ | 1.89 | |
| LP(3)$O_{20}$ → π*$C_4$-$N_5$ | 3.02 | |
| LP(1)$O_{20}$ → π*$C_6$-$N_7$ | 1.34 | 9 |
| LP(2)$O_{20}$ → π*$C_6$-$N_7$ | 0.80 | |
| LP(1)$O_{20}$ → π*$C_8$-$N_9$ | 1.39 | 10 |
| LP(2)$O_{20}$ → π*$C_8$-$N_9$ | 0.88 | |
| LP(1)$O_{20}$ → π*$C_{10}$-$N_{11}$ | 1.81 | 30 |
| LP(2)$O_{20}$ → π*$C_{10}$-$N_{11}$ | 1.76 | |
| LP(3)$O_{20}$ → π*$C_{10}$-$N_{11}$ | 3.32 | |
| Total n→π* energy | 17.97 | 78 |
| LP(1)$O_{20}$ → σ*$C_1$-$C_2$ | 1.47 | 11 |
| LP(3)$O_{20}$ → σ*$C_1$-$C_2$ | 1.18 | |
| LP(1)$O_{20}$ → σ*$C_2$-$C_3$ | 1.42 | 11 |
| LP(3)$O_{20}$ → σ*$C_2$-$C_3$ | 1.09 | |
| Total C-bond energy | 5.16 | 22 |
| Total donor-acceptor energy | 23.13 | -- |

**QTAIM Analysis:**

The QTAIM analysis was performed with the wave function obtained at the MP2/def2-TZVPP level of theory. The molecular graph shows only one bond critical point between the PNO-O with the nearest carbon atom, i.e., the carbon atom of the cyclopropane ring, which is an indicator of the C-bond with only one carbon atom of DMTCCP. The characteristics of the bond critical point (BCP) i.e., the electron density (ρ) and the laplacian of the electron density ($\nabla^2\rho$), follow the criteria mentioned by Koch and Popelier.[17] But the molecular graph does not show any BCP for the n→π* interaction. This is because the bond path is shown between the two closest atoms. More than two bond critical points lead to a ring critical point (RCP). In this heterodimer, it seems that the BCPs between the O atom of PNO and C atoms of DMTCCP and the RCPs are in close proximity. To avoid the coalescence of BCPs and RCPs, only one BCP is shown. This is also reflected in the mutual penetration of the interacting atomic pairs, as short distances lead to high mutual penetration. The values for the mutual penetration are

given below in **Table S2**. However, the positive values of the mutual penetration also confirm the presence of the noncovalent interaction between PNO and DMTCCP.[18] We have provided the distances between the carbon atoms of DMTCCP and the oxygen atom of PNO in **Figure S2** and the molecular graph of the PNO-DMTCCP complex in **Figure S3**.

**Table S2:** Mutual penetration for the interacting atomic pairs.

| Interacting atomic pairs | Mutual Penetration (a.u.) |
|---|---|
| O20•••C1 | 1.34 |
| O20•••C3 | 1.33 |
| O20•••C4 | 1.22 |
| O20•••C6 | 0.87 |
| O20•••C8 | 0.88 |
| O20•••C10 | 1.23 |

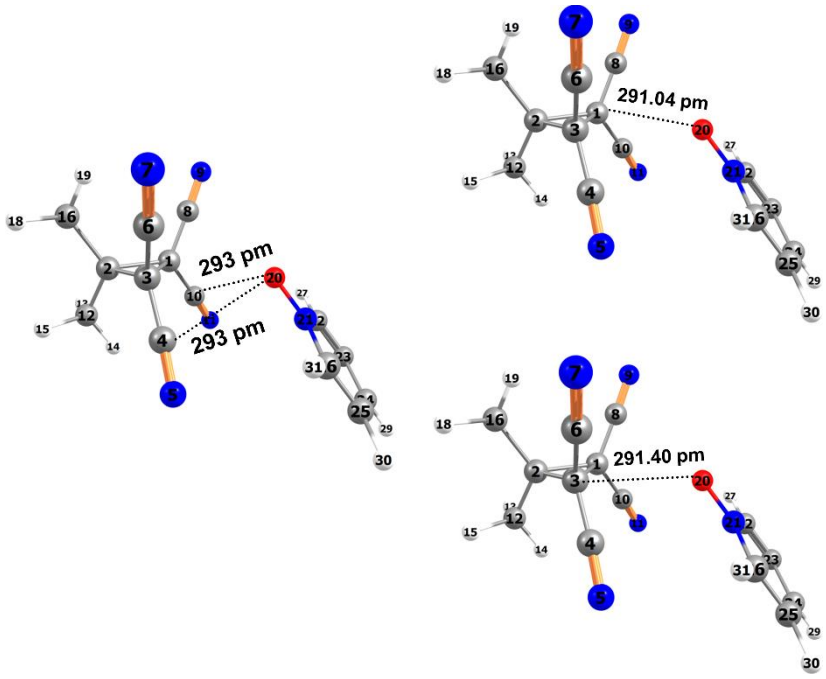


**Figure S2:** Distances between the PNO-O atom and the carbon atoms involved in the n→σ* and n→π* interactions.

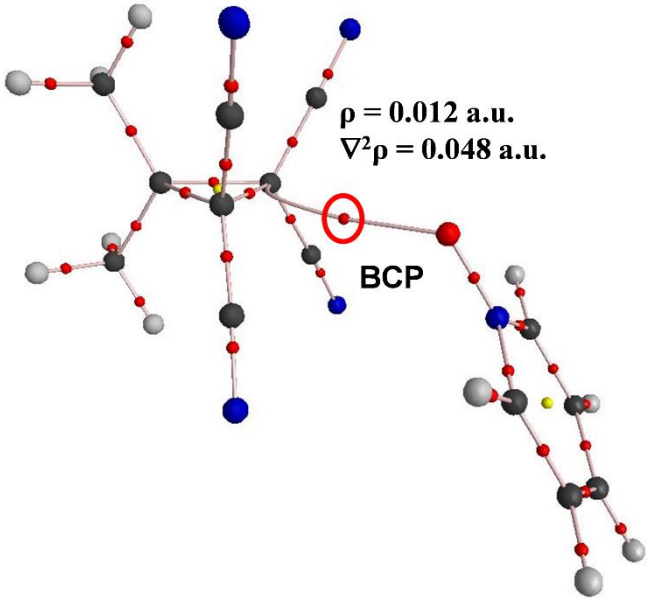


**Figure S3:** Molecular graph of the PNO-DMTCCP complex with the characteristics parameters of the BCP suggests the presence of the C-bond.

## Experimental Details

### Materials and method:

Acetone, malononitrile, sodium acetate, ethanol, and bromine solution were used without further purification to synthesize DMTCCP following the method described by Heywood et al.[19]. To characterize the DMTCCP, and we used $^{1}H$ (400 MHz) and $^{13}C$ (100 MHz) NMR spectroscopy.

The $^{1}H$-NMR spectrum of DMTCCP shows a peak at 1.80 ppm for the methyl groups. The peak at 1.55 ppm is due to the water in $CDCl_3$, which was taken care of while performing the concentration- and temperature-dependent experiments by drying the solvent over the molecular sieves. The $^{13}C$-NMR spectrum of DMTCCP shows peaks at 108.13 ppm for $\underline{C}N$, 41.00 ppm for $\underline{C}(CN)_2$, 25.95 ppm for $\underline{C}(CH_3)_2$, and 20.23 ppm for $\underline{C}H_3$ group.

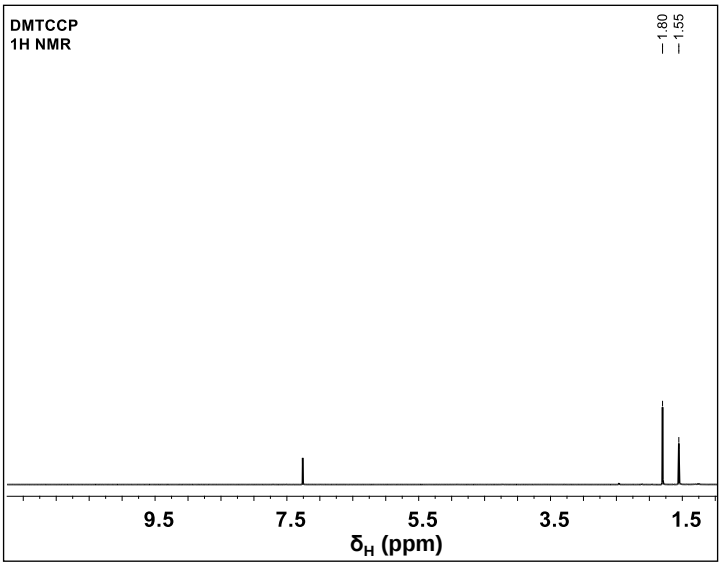


**Figure S4:** $^{1}H$-NMR spectrum of DMTCCP

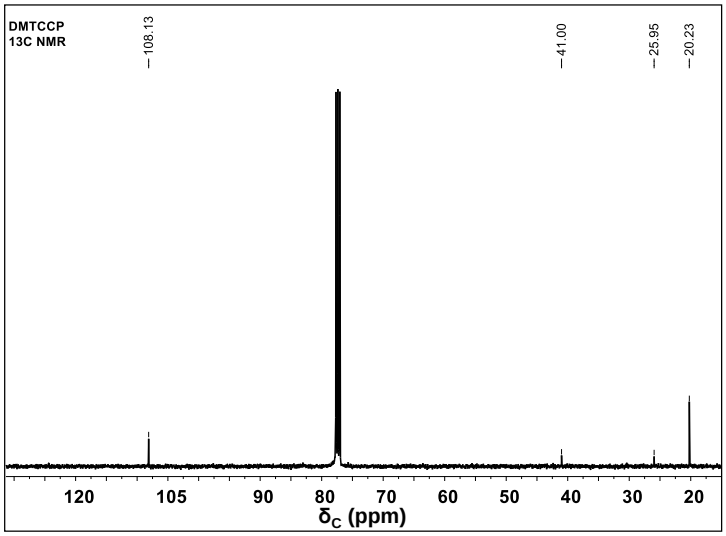


**Figure S5:** $^{13}C$-NMR spectrum of DMTCCP

We would like to mention that both solutes are present in the solid state, and while performing the experiments, they were taken in milligrams, which hardly alters the total volume. Subsequently, the density and polarity of the solvent remain unaffected. We measured the viscosities of the $CDCl_3$, DMTCCP in the $CDCl_3$, and PNO in $CDCl_3$ at 21°C. The measured viscosities were 0.47 cP for all the cases.

**NMR experiment details to evaluate the strength of the interaction**

$CDCl_3$ was used as a solvent for NMR experiments. All NMR studies (except DOSY) were conducted using a Bruker Avance-III HD liquid state 400 MHz NMR spectrometer equipped with a triple-channel cryoprobe equipped with z-gradients.

**Concentration-dependent NMR details**

We performed the concentration-dependent NMR titration with a fixed concentration of DMTCCP at 0.03M with a varying concentration of PNO from 75mM to 2M. The temperature of the experiment was fixed at 298K. We fitted the data into the following equation to find out the equilibrium constant of the interaction and thus, the change in Gibb's free energy.

$$\boldsymbol{\delta_{obs} = \delta_{H_0} + (\Delta\delta \times y)} \quad \textbf{(S4)}$$

**where,**

$$\boldsymbol{y = \frac{\{1 + k([H]_0 + [G]_0)\} - [\{1 + k([H]_0 + [G]_0)\}^2 - (4k^2[H]_0[G]_0)]^{1/2}}{2k[H]_0}}$$

$\delta_{obs}$ is the observed chemical shift, $\delta_{H0}$ is the chemical shift when only host (DMTCCP) is present, $\Delta\delta$ is the difference between the final chemical shift and initial chemical shift, $[H]_0$ is the initial concentration of the host, $[G]_0$ is the total concentration of the guest (PNO), i.e., free PNO molecules and complexed PNO molecules, and k is the equilibrium constant of the following equilibrium:

$$H + G \rightleftharpoons HG$$

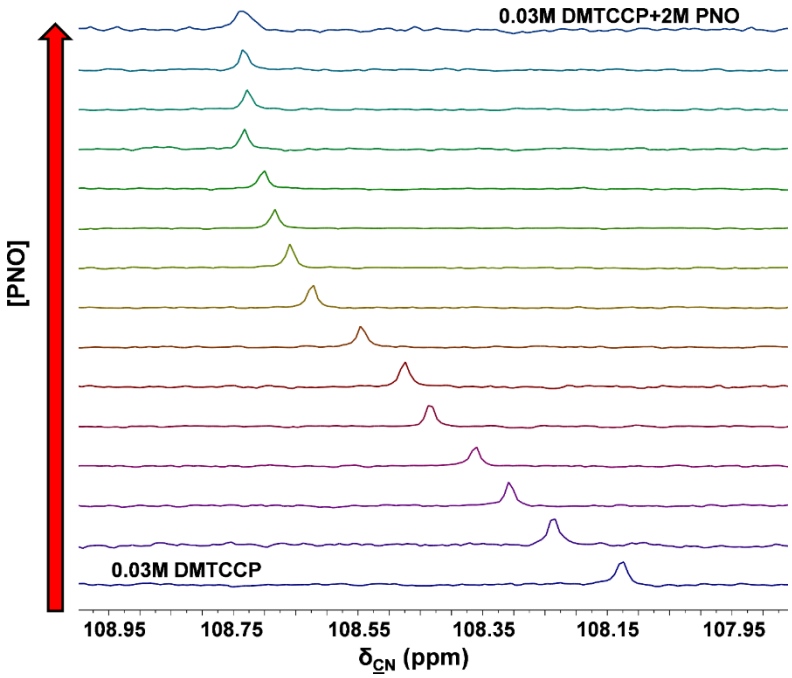


***Figure S6:*** *Concentration-dependent $^{13}$C-NMR spectra at 298K.*

In the concentration-dependent $^{13}$C-NMR we observed a downfield chemical shift of the nitrile carbon upon increasing the concentration of the PNO. Now, when we added PNO to the solution of DMTCCP, due to the n→π* interaction, we observed the downfield shift. After that, as we added more PNO, the chemical shift observed is due to the combined chemical shifts of the monomer (DMTCCP) and the dimer (PNO-DMTCCP ) as follows:

$$\delta_{obs} = x_{DMTCCP} * \delta_{DMTCCP} + (1-x_{DMTCCP}) * \delta_{PNO\text{-}DMTCCP}$$

where $x_{DMTCCP}$ is the fraction of DMTCCP molecules present in the solution and $(1-x_{DMTCCP})$ denotes the fraction of complex (PNO-DMTCCP ) present in the solution.

Again, why we are observing a downfield chemical shift instead of an upfield chemical shift upon complex formation can be described from the σ→π* energy gap of the C=O or C≡N bond.[20] Lesser the gap, the more is chemical shift value. To explain this, we conducted Natural Localised Molecular Orbital (NLMO) analysis. It shows that the average σ→π* energy gap for C≡N in DMTCCP is 1.142. In contrast, the same in DMTCCP-PNO is 1.128, which suggests that the σ→π* energy gap of the C≡N bond decreases by 0.014, leading to the downfield shift.

**Temperature-dependent NMR details**

We performed the temperature-dependent NMR with a 0.03M DMTCCP-1.5M PNO solution by varying the temperature from 233K to 313K. We fitted the data into the following equation to get the change in enthalpy for the interaction.

$$\boldsymbol{\delta_{obs} = \delta_{H_0} + (\Delta\delta \times y)} \quad \textbf{(S5)}$$

**where,**

$$y = \frac{\left\{1 + e^{-\left(\frac{\Delta H - T\Delta S}{RT}\right)}([H]_0 + [G]_0)\right\} - \left[\left\{1 + e^{-\left(\frac{\Delta H - T\Delta S}{RT}\right)}([H]_0 + [G]_0)\right\}^2 - \left(4e^{-2\left(\frac{\Delta H - T\Delta S}{RT}\right)}[H]_0[G]_0\right)\right]^{1/2}}{2e^{-\left(\frac{\Delta H - T\Delta S}{RT}\right)}[H]_0}$$

ΔH and ΔS are the enthalpy change and entropy change for dimer formation, respectively. R is the universal gas constant, and T is the temperature.

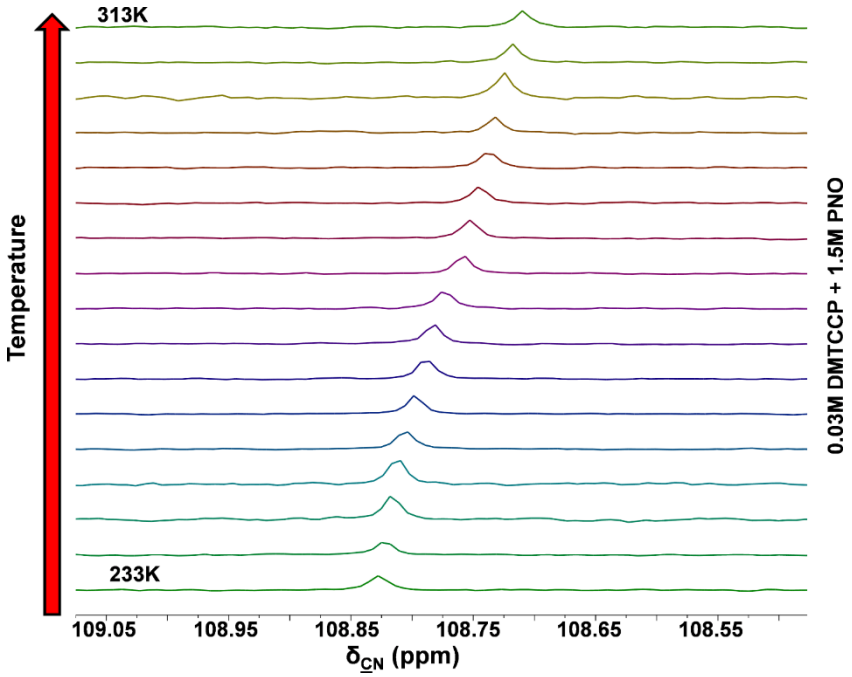


***Figure S7:*** *Temperature-dependent $^{13}$C-NMR experiment with 0.03M DMTCCP–1.5M PNO solution.*

**DOSY experiments details**

Translational diffusion measurements[21] were performed using the Pulse field Gradient Stimulated Echo (PGSE) method with bipolar gradients to reduce the effect of Eddy current in the 700MHz NMR machine. The diffusion experiments were performed with 8 scans for each gradient strength and with 16 different gradient strengths varied linearly from 5% to 95% of

the maximum gradient strength, 48.15 Gauss/cm being the peak gradient value. Recycle delay was 5s, duration of gradient pulses was 1 ms, while the diffusion delay of 30 ms and 40 ms were used for DMTCCP and DMTCCP+PNO samples, respectively. The concentration of DMTCCP was kept at 0.03M for both monomer and complex. The concentration of PNO taken in the mixture was 1.5M, i.e., 0.03M DMTCCP-1.5M PNO solution was taken for the complex.

**Cartesian Coordinates of the Optimized Structures (in Å)**

**PNO-DMTCCP (in gas phase)**

| | | | |
|---|---|---|---|
| C | 1.711915900 | 0.637942500 | 0.511470300 |
| C | 2.989946900 | -0.083267500 | 0.035219200 |
| C | 1.634480300 | -0.543952500 | -0.536371500 |
| C | 1.065897700 | -1.789888800 | -0.080429800 |
| N | 0.666316700 | -2.813861300 | 0.288874000 |
| C | 1.293825200 | -0.211495300 | -1.898855500 |
| N | 1.076309300 | 0.040193900 | -3.009497200 |
| C | 1.441810800 | 1.973194800 | 0.035384800 |
| N | 1.285391100 | 3.057556200 | -0.343427000 |
| C | 1.205204900 | 0.371231700 | 1.836594000 |
| N | 0.852057500 | 0.145332200 | 2.917258300 |
| C | 3.694864400 | -1.000602400 | 1.014918900 |
| H | 4.378365300 | -0.408464800 | 1.632048800 |
| H | 3.006432400 | -1.533791100 | 1.673465300 |
| H | 4.281657400 | -1.737134800 | 0.456343200 |
| C | 3.923348700 | 0.675806600 | -0.887779100 |
| H | 4.606502800 | 1.282876900 | -0.284997800 |
| H | 4.514812000 | -0.039283000 | -1.468851000 |
| H | 3.396251800 | 1.333472300 | -1.581647100 |
| O | -1.075616200 | 0.281628300 | -0.125044800 |
| N | -2.337222900 | 0.089408000 | -0.049433300 |
| C | -2.897452200 | -0.456379100 | 1.083025000 |
| C | -4.263647000 | -0.662389800 | 1.175271800 |
| C | -5.106568000 | -0.322334400 | 0.113771200 |
| C | -4.526894800 | 0.227932800 | -1.032658600 |
| C | -3.158648300 | 0.426536300 | -1.101239000 |
| H | -2.178382100 | -0.693972300 | 1.857074900 |
| H | -4.658429900 | -1.094070300 | 2.090470200 |
| H | -6.178380500 | -0.480074800 | 0.177449100 |
| H | -5.131742500 | 0.510825000 | -1.889414500 |
| H | -2.632165800 | 0.846979600 | -1.948878800 |

**PNO-DMTCCP (in $CHCl_3$)**

| | | | |
|---|---|---|---|
| C | 1.565129200 | 0.721574200 | 0.458433000 |
| C | 2.771011700 | -0.123851100 | -0.002386700 |
| C | 1.507752600 | -0.099563900 | -0.888756300 |
| C | 0.634853000 | -1.248053000 | -0.915124900 |
| N | -0.019876300 | -2.204558200 | -0.928967700 |
| C | 1.515921300 | 0.649185500 | -2.121298500 |

| | | | |
|---|---|---|---|
| N | 1.563336900 | 1.241738900 | -3.116057500 |
| C | 1.621668000 | 2.158986300 | 0.355653500 |
| N | 1.709767600 | 3.312018700 | 0.280518500 |
| C | 0.739153100 | 0.251232500 | 1.543851400 |
| N | 0.122670400 | -0.150282200 | 2.439683100 |
| C | 3.070525300 | -1.397163800 | 0.760908800 |
| H | 3.691492100 | -1.152533500 | 1.627913500 |
| H | 2.171804400 | -1.909966900 | 1.109809800 |
| H | 3.629927700 | -2.076430400 | 0.110684400 |
| C | 3.996301100 | 0.612259700 | -0.503200200 |
| H | 4.627593300 | 0.871175300 | 0.352120800 |
| H | 4.560505600 | -0.050014500 | -1.166684600 |
| H | 3.754999300 | 1.527630200 | -1.047801700 |
| O | -1.146309200 | 1.054365400 | -0.545591400 |
| N | -2.229375800 | 0.486980500 | -0.131437900 |
| C | -2.762691700 | 0.815178800 | 1.089795600 |
| C | -3.921435600 | 0.211512100 | 1.548683100 |
| C | -4.571087700 | -0.750949000 | 0.771456400 |
| C | -4.018847500 | -1.076465700 | -0.470188300 |
| C | -2.859151100 | -0.456405600 | -0.904069300 |
| H | -2.202162300 | 1.563560000 | 1.633684200 |
| H | -4.304093900 | 0.504209200 | 2.521661100 |
| H | -5.479084000 | -1.231012200 | 1.121584500 |
| H | -4.479545300 | -1.817038100 | -1.116805400 |
| H | -2.370511300 | -0.657365000 | -1.847955400 |

**PNO Dimer (in $CHCl_3$)**

| | | | |
|---|---|---|---|
| O | -1.7537635 | 0.3191085 | 0.1170781 |
| N | -2.8752316 | -0.1919540 | -0.2614588 |
| C | -2.9214744 | -1.4454402 | -0.8251548 |
| C | -4.1265435 | -1.9995591 | -1.2263495 |
| C | -5.3233769 | -1.2950678 | -1.0696769 |
| C | -5.2620654 | -0.0202269 | -0.5003587 |
| C | -4.0457620 | 0.5121029 | -0.1060495 |
| H | -1.9582273 | -1.9362112 | -0.9274609 |
| H | -4.1112059 | -2.9931648 | -1.6646474 |
| H | -6.2705447 | -1.7235366 | -1.3811146 |
| H | -6.1571969 | 0.5773327 | -0.3548887 |
| H | -3.9194554 | 1.4898338 | 0.3419971 |
| O | -0.0450260 | -3.0121832 | -1.5685316 |
| N | 1.0636270 | -2.3683392 | -1.4319943 |
| C | 2.2344646 | -2.8871490 | -1.9323183 |
| C | 3.4365361 | -2.2135954 | -1.7909434 |
| C | 3.4829856 | -0.9820683 | -1.1318574 |

| | | | |
|---|---|---|---|
| C | 2.2858967 | -0.4629056 | -0.6312109 |
| C | 1.0955013 | -1.1550087 | -0.7855605 |
| H | 2.1206292 | -3.8429061 | -2.4286741 |
| H | 4.3326971 | -2.6673888 | -2.2037118 |
| H | 4.4190213 | -0.4458151 | -1.0134971 |
| H | 2.2587070 | 0.4909080 | -0.1122789 |
| H | 0.1328668 | -0.8025843 | -0.4277198 |

**DMTCCP Dimer**

| | | | |
|---|---|---|---|
| C | 2.7606525 | 0.9691687 | 1.4590209 |
| C | 3.3920321 | -0.1468312 | 0.6064399 |
| C | 1.8608623 | -0.1725566 | 0.8106985 |
| C | 1.2802985 | -1.1410837 | 1.7076870 |
| N | 0.8325785 | -1.9301965 | 2.4289920 |
| C | 0.9924297 | 0.2116063 | -0.2746121 |
| N | 0.3112923 | 0.5171246 | -1.1612545 |
| C | 2.6290450 | 2.2978340 | 0.9138583 |
| N | 2.5246659 | 3.3604139 | 0.4636256 |
| C | 2.9204577 | 0.9423559 | 2.8918964 |
| N | 3.0597944 | 0.9050300 | 4.0417963 |
| C | 4.2112273 | -1.1996708 | 1.3225989 |
| H | 5.2329112 | -0.8304418 | 1.4394908 |
| H | 3.8195550 | -1.4547265 | 2.3096091 |
| H | 4.2332165 | -2.1065437 | 0.7112936 |
| C | 3.9118280 | 0.2297509 | -0.7646620 |
| H | 4.9266877 | 0.6207428 | -0.6541230 |
| H | 3.9425434 | -0.6675883 | -1.3894650 |
| H | 3.3001701 | 0.9835874 | -1.2650419 |
| C | 7.8218132 | 2.3271318 | 3.3048005 |
| C | 7.6475300 | 2.0940980 | 4.8210271 |
| C | 8.4205483 | 1.0315413 | 4.0125252 |
| C | 7.7856687 | -0.2253452 | 3.6994890 |
| N | 7.2559364 | -1.2257022 | 3.4503283 |
| C | 9.8555082 | 0.9501641 | 4.1310654 |
| N | 11.0076891 | 0.8964147 | 4.2443096 |
| C | 8.7594637 | 3.3172278 | 2.8363365 |
| N | 9.5148725 | 4.1204922 | 2.4794451 |
| C | 6.7003381 | 2.1162582 | 2.4237102 |
| N | 5.7879909 | 1.9294347 | 1.7346434 |
| C | 6.2655588 | 1.7294558 | 5.3202345 |
| H | 5.6911428 | 2.6474513 | 5.4731705 |
| H | 5.7098512 | 1.0863200 | 4.6357657 |
| H | 6.3621914 | 1.2137840 | 6.2800957 |
| C | 8.4451966 | 2.9769044 | 5.7581872 |

H 7.8890211 3.9036270 5.9267301
H 8.5607064 2.4593914 6.7149485
H 9.4365469 3.2289279 5.3755165

**References**


1. C. I. Bayly, P. Cieplak, W. Cornell and P. A. Kollman, *J. Phys. Chem.*, 1993, **97**, 10269-10280.
2. G. W. T. M. J. Frisch, H. B. Schlegel, G. E. Scuseria, M. A. Robb, J. R. Cheeseman, G. Scalmani, V. Barone, B. Mennucci, G. A. Petersson, H. Nakatsuji, M. Caricato, X. Li, H. P. Hratchian, A. F. Izmaylov, J. Bloino, G. Zheng, J. L. Sonnenberg, M. Hada, M. Ehara, K. Toyota, R. Fukuda, J. Hasegawa, M. Ishida, T. Nakajima, Y. Honda, O. Kitao, H. Nakai, T. Vreven, J. A. Montgomery, Jr., J. E. Peralta, F. Ogliaro, M. Bearpark, J. J. Heyd, E. Brothers, K. N. Kudin, V. N. Staroverov, R. Kobayashi, J. Normand, K. Raghavachari, A. Rendell, J. C. Burant, S. S. Iyengar, J. Tomasi, M. Cossi, N. Rega, J. M. Millam, M. Klene, J. E. Knox, J. B. Cross, V. Bakken, C. Adamo, J. Jaramillo, R. Gomperts, R. E. Stratmann, O. Yazyev, A. J. Austin, R. Cammi, C. Pomelli, J. W. Ochterski, R. L. Martin, K. Morokuma, V. G. Zakrzewski, G. A. Voth, P. Salvador, J. J. Dannenberg, S. Dapprich, A. D. Daniels, Ö. Farkas, J. B. Foresman, J. V. Ortiz, J. Cioslowski, and D. J. Fox, Gaussian 09, 2009.
3. J. Wang, W. Wang, P. A. Kollman and D. A. Case, *J. Mol. Graph. Model.*, 2006, **25**, 247-260.
4. V. B. D.A. Case, J.T. Berryman, R.M. Betz, Q. Cai, D.S. Cerutti, T.E. Cheatham, III, T.A. Darden, R.E. Duke, H. Gohlke, A.W. Goetz, S. Gusarov, N. Homeyer, P. Janowski, J. Kaus, I. Kolossváry, A. Kovalenko, T.S. Lee, S. LeGrand, T. Luchko, R. Luo, B. Madej, K.M. Merz, F. Paesani, D.R. Roe, A. Roitberg, C. Sagui, R. Salomon-Ferrer, G. Seabra, C.L. Simmerling, W. Smith, J. Swails, R.C. Walker, J. Wang, R.M. Wolf, X. Wu and P.A. Kollman, *AMBER14*, 2014.
5. J. Wang, R. M. Wolf, J. W. Caldwell, P. A. Kollman and D. A. Case, *J. Comput. Chem.*, 2004, **25**, 1157-1174.
6. U. Essmann, L. Perera, M. L. Berkowitz, T. Darden, H. Lee and L. G. Pedersen, *J. Chem. Phys.*, 1995, **103**, 8577-8593.
7. J.-P. Ryckaert, G. Ciccotti and H. J. C. Berendsen, *J. Comput. Phys.*, 1977, **23**, 327-341.
8. J. A. Izaguirre, D. P. Catarello, J. M. Wozniak and R. D. Skeel, *J. Chem. Phys.*, 2001, **114**, 2090-2098.
9. D. R. Roe and T. E. Cheatham, *J. Chem. Theory Comput.*, 2013, **9**, 3084-3095.
10. M. Brehm and B. Kirchner, *J. Chem. Inf. Model.*, 2011, **51**, 2007-2023.
11. J. Wang and T. Hou, *J. Comput. Chem.*, 2011, **32**, 3505-3519.
12. *TURBOMOLE V7.2, 2017 University of Karlsruhe and Forschungszentrum Karlsruhe GmbH*, 1989-2007.
13. R. K. Dennington, Todd A.; Millam, John M., 2016.
14. J. P. Foster and F. Weinhold, *J. Am. Chem. Soc.*, 1980, **102**, 7211-7218.
15. G. W. T. M. J. Frisch, H. B. Schlegel, G. E. Scuseria, M. A. Robb, J. R. Cheeseman, G. Scalmani, V. Barone, G. A. Petersson, H. Nakatsuji, X. Li, M. Caricato, A. V. Marenich, J. Bloino, B. G. Janesko, R. Gomperts, B. Mennucci, H. P. Hratchian, J. V. Ortiz, A. F. Izmaylov, J. L. Sonnenberg, D. Williams-Young, F. Ding, F. Lipparini, F. Egidi, J. Goings, B. Peng, A. Petrone, T. Henderson, D. Ranasinghe, V. G. Zakrzewski, J. Gao, N. Rega, G. Zheng, W. Liang, M. Hada, M. Ehara, K. Toyota, R. Fukuda, J.

Hasegawa, M. Ishida, T. Nakajima, Y. Honda, O. Kitao, H. Nakai, T. Vreven, K. Throssell, J. A. Montgomery, Jr., J. E. Peralta, F. Ogliaro, M. J. Bearpark, J. J. Heyd, E. N. Brothers, K. N. Kudin, V. N. Staroverov, T. A. Keith, R. Kobayashi, J. Normand, K. Raghavachari, A. P. Rendell, J. C. Burant, S. S. Iyengar, J. Tomasi, M. Cossi, J. M. Millam, M. Klene, C. Adamo, R. Cammi, J. W. Ochterski, R. L. Martin, K. Morokuma, O. Farkas, J. B. Foresman, and D. J. Fox, Gaussian 16, 2016.

16. V. R. Mundlapati, S. Gautam, D. K. Sahoo, A. Ghosh and H. S. Biswal, *J. Phys. Chem. Lett.*, 2017, **8**, 4573-4579.
17. U. Koch and P. L. A. Popelier, *J. Phys. Chem. A*, 1995, **99**, 9747-9754.
18. D. Mani and E. Arunan, *Phys. Chem. Chem. Phys.*, 2013, **15**, 14377-14383.
19. V. L. Heywood, T. P. J. Alford, J. J. Roeleveld, S. J. Lekanne Deprez, A. Verhoofstad, J. I. van der Vlugt, S. R. Domingos, M. Schnell, A. P. Davis and T. J. Mooibroek, *Chem. Sci.*, 2020, **11**, 5289-5293.
20. D. K. Sahoo, S. Jena, J. Dutta, S. Chakrabarty and H. S. Biswal, *ACS Cent. Sci.*, 2018, **4**, 1642-1651.
21. K. F. Morris and C. S. Johnson, *J. Am. Chem. Soc.*, 1992, **114**, 3139-3141.